An Investigation into the Dominant Reactions for Ethylene Destruction in Non-Thermal Atmospheric Plasmas

Robby Aerts,* Xin Tu, Christophe De Bie, J. Christopher Whitehead, Annemie Bogaerts

A crucial step, which is still not well understood in the destruction of volatile organic compounds (VOCs) with low temperature plasmas, is the initiation of the process. Here, we present a kinetic model for the destruction of ethylene in low temperature plasmas that allows us to calculate the relative importance of all plasma species and their related reactions. Modifying the ethylene concentration and/or the SED had a major impact on the relative importance of the radicals (i.e., mainly atomic oxygen) and the metastable nitrogen (i.e., more specifically $N_2(A^3\Sigma_u^+)$) in the destruction process. Our results show that the direct destruction by electron impact reactions for ethylene can be neglected; however, we can certainly not neglect the influence of $N_2(A^3\Sigma_u^+)$).
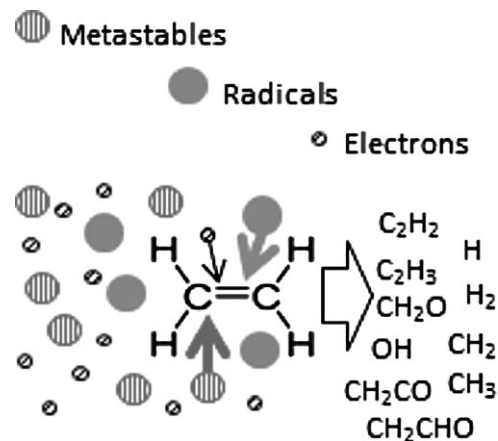
1. Introduction

Commonly used pollution control technologies, such as thermal and catalytic oxidation, which are operated at temperatures above 400 °C, are considered as energy inefficient because of their need to heat up the complete gas mixture. A possible alternative technology is the destruction of pollutants by low temperature plasma such as dielectric barrier discharges (DBDs) and corona discharges.[1–4] They transfer most of their energy to the electrons which will generate other active species such as metastables and radicals with little gas heating.

The use of dielectric barrier discharges for the control of gaseous pollutants was addressed by several researchers, with first publications in the beginning of the 1990s.[5–10] Kogelschatz divided these pollutants in 3 different subgroups, i.e., the treatment of volatile organic compounds (VOCs), the treatment of diesel exhaust gases and greenhouse gas abatement.[11] The present paper will focus on the treatment of VOCs, which are pollutants diluted in air. Nowadays more and more papers are published for the plasma abatement of VOCs, presenting advanced reactor configurations, including packed bed reactors, the combination of plasma with catalyst in so-called

R. Aerts, C. De Bie, Prof. A. Bogaerts
Research Group PLASMANT, Department of Chemistry, University of Antwerp, Universiteitsplein 1, 2610 Wilrijk, Belgium
E-mail: robby.aerts@ua.ac.be
Dr. X. Tu
Department of Electrical Engineering and Electronics, The University of Liverpool, Liverpool, L69 3GJ, UK
Prof. J. C. Whitehead
School of Chemistry, The University of Manchester, Oxford Road, Manchester, M13 9PL, UK

plasma catalysis, and even microplasma reactors with and without catalyst.[12–14] Each of these configurations demonstrated an improvement in terms of removal and energy efficiency; however, the total performance gap between plasma technology and the conventional destruction technology is still too small to be a competitive alternative.

In order to obtain more insight into the destruction process of VOCs, we present a kinetic model for the destruction of ethylene, taking into account reactions by radicals, metastables as well as electrons. Indeed, ethylene is a well-known and widely investigated hydrocarbon in plasma and combustion science.[15–19] Ethylene is considered here as a case study but the results could also be used as a guideline for other hydrocarbons or VOCs. In this paper, we will show the influence of electrons, metastable nitrogen and radicals on the destruction process at different concentrations of ethylene and at different values of specific energy deposition (SED).

An understanding of the destruction process can help us to improve the general efficiency of the process and can enforce the synthesis of suitable catalysts for plasma catalysis applications. A crucial step in the destruction process of VOCs is the initiation step, where the reactions with the VOC itself occur. This process is in most cases not well known and therefore many authors suggest different types of dominant reactions. Some authors suggest direct electron impact dissociation as one of the dominant destruction reactions, but also dissociation reactions induced by metastables and radicals are believed to be dominant destruction mechanisms.[20–30] As far as we know, no comparative investigation has been carried out before to support these assumptions.

2. Experimental Section

2.1. Description of the Model

The model used in this work is a global (0D) model, called global_kin, developed by Dorai and Kushner,[31] which consists of two major parts. The first part is a Boltzmann solver which uses the cross sections for the electron induced reactions and constructs lookup tables for the reaction rate coefficients versus the mean electron energy. The second part is the gas phase kinetics module which calculates the changes in density of every species and the changes in energy of the electrons. To describe the complete destruction process of ethylene in dry air (79% N_2 and 21% O_2), a chemistry set has been built with 545 reactions and 103 species. A list of species, the reactions for the simplified air chemistry and some important reactions between metastable nitrogen and ethylene are available in the Supporting Information.

To identity the important reactions, a brief summary of the mechanism for the destruction of ethylene is presented here. Most of the initial destruction of ethylene is caused by reactions with

atomic oxygen to form products like CH_2, CH_3 and CHO radicals but also stable molecules, such as formaldehyde. Formaldehyde is also mentioned as one of the major by-products in other papers involving ethylene destruction by plasma;[32,33] on its turn it will react with OH radicals to form CHO radicals, which finally react further to form CO and CO_2. Our simulations predict that the CHO radicals are the controlling reactants for the selectivity of CO and CO_2, together with the oxidation of CO to CO_2 by atomic oxygen. An alternative destruction pathway, is the destruction by reaction with nitrogen metastable molecules to C_2H_2 and to C_2H_3 radicals. These species will then react with atomic oxygen or molecular oxygen to form formaldehyde which reacts further to CO and CO_2 as discussed above. One other possible mechanism, but less likely, is the direct destruction by electron impact dissociation reactions, which can also produce C_2H_2 and C_2H_3 radicals.

The metastable molecules represent both the $N_2(A^3\Sigma_u^+)$ and $N_2(a'\Sigma_u^-)$ species, whereas the radicals playing a role in the ethylene destruction, include atomic oxygen, OH and CH_3 radicals, and H atoms.

A DBD is typically characterized by many current pulses (or streamers); however, we do not know the exact number of pulses each molecule passes per time and modelling streamer formation is beyond the scope of this paper. In literature, two different energy deposition systems are typically assumed in zero dimensional plasma modelling of dielectric barrier discharges. The first one assumes a uniform processing of the gas as it passes through the reactor. During each half-cycle, the microdischarge current pulses create active species which then will initiate or continue the chemistry.[34,35] This method does not only describe a current pulse and an afterglow but also accumulation effects of certain radicals as a function of time, which is also the case in realistic DBDs. The second method describes only one current pulse and therefore neglects the accumulation by repetition of the pulses.[36] In this paper, we have applied the second method, to focus on the initiation process during one pulse. We have, however, also applied the first method to investigate its influence on the destruction efficiency of ethylene. It became clear that this first method resulted in an unrealistically high removal efficiency (RE) in certain cases. Indeed, during each half cycle, active species are created, but in reality not every molecule passes the same number of current pulses (streamers) and obviously, this method therefore yielded an overestimation of the RE in these cases. In fact, for a realistic description of the destruction process, a good estimate of the number of pulses (streamers) in a DBD would be necessary. As we are only interested in the detailed chemistry of one current pulse to indicate the effect of short living species, such as metastables and electrons, on the initiation step, we only show results for one current pulse of 200 ns with a rise and fall time of 10 ns, followed by an afterglow of almost 1 ms at a gas temperature of 300 K. The electron density is calculated to be in the order of 10^{12} cm^{-3} at a SED of 5 mJ · cm^{-3} and 10^{15} cm^{-3} at a SED of 2 500 mJ · cm^{-3}, which is in reasonable agreement with literature.[31,36] However, we also performed simulations with a multi-pulsed energy deposition of 10 ns pulses and a frequency of 7.35 Hz. This simulation indicated only a slight increase in RE by 1% caused by accumulation of atomic oxygen. Other accumulating species like ozone and NO$_x$ were also found in higher densities compared to one pulse but did not influence the RE.

2.2. Description of the Experiments

The experimental setup used for validation is a cylindrical DBD reactor consisting of two coaxial fused quartz tubes, both of which are covered by a stainless steel mesh electrode. A more detailed description of the reactor can be found in Tu et al.[37] without a catalyst inside the reactor and a gap of 3 mm instead of 4.5 mm. The reactor volume is 11.4 cm^3 and the experiments are carried out at a constant flow rate of 1 slm at 300 K which corresponds to a residence time of 0.684 s. The gases are analysed by a two-channel microgas chromatography (Agilent 3000A) equipped with two thermal conductivity detectors (TCD). The first channel contains a Molecular Sieve 5A column for the separation of H$_2$, CO and CH$_4$, while the second channel is equipped with a Poraplot Q column for the measurement of CO$_2$ and C$_2$–C$_4$ hydrocarbons. The gas chomatograph is calibrated for a wide range of concentrations for each gaseous component using reference gas mixtures (Agilent Universal Gas Mixture) and other calibrated gas mixes. All the electrical signals are sampled by a four-channel digital oscilloscope (Agilent DSO6014A, 2 GHz). To measure the discharge power an online real-time measurement based on LABVIEW is used for calculation of the Q–U Lissajous figures.

3. Results and Discussion

3.1. Validation of the Model

In order to validate the model, simulations and experiments were performed for concentrations of 3 500, 8 700 and 13 700 ppm ethylene in dry air as a function of the SED. The upper graph in Figure 1 presents the RE from the experiment and the simulations for the three different concentrations mentioned above. The RE is defined as:

$$\text{Removal efficiency } (\%) = \text{RE } (\%)$$
$$= \frac{C_2H_{4\,\text{inlet}} - C_2H_{4\,\text{outlet}}}{C_2H_{4\,\text{inlet}}} \tag{1}$$

The figure shows a reasonable agreement between the simulations and the experiment for the different values of SED and ethylene concentration. An almost complete destruction is reached at 2 500 mJ · cm^{-3} for 3 500 and 8 700 ppm ethylene; the highest concentration of 13 700 ppm requires a slightly higher SED for complete destruction, i.e., around 2 750 mJ · cm^{-3}. It should be mentioned that a stable plasma could not be obtained experimentally at lower values of SED and therefore the ethylene concentration was chosen here to be higher than commonly used concentrations in VOC treatment (which are typically below 1 000 ppm). However, for the validation of the model at lower values of concentration and SED, a comparison with results adopted from literature in NO$_x$ abatement has been presented in the bottom graph of Figure 1. The bottom graph presents the density of ethylene and NO, as obtained by our simulations compared with the
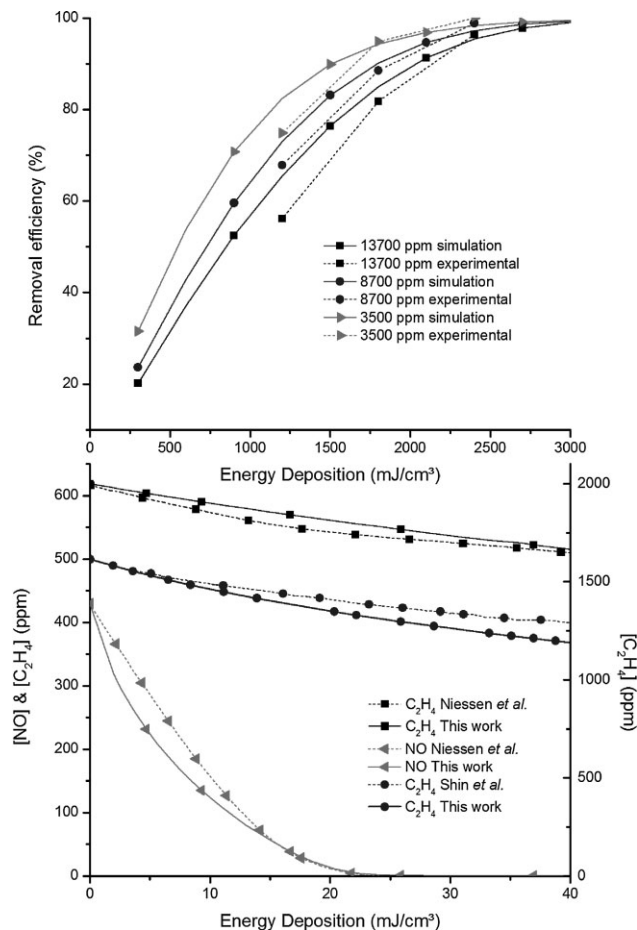
Figure 1. Top graph presents a comparison between the simulations and the experiments for the RE as a function of the specific energy density (SED) at 13 700, 8 700 and 3 500 ppm ethylene in dry air at a gas temperature of 300 K. The bottom graph presents a comparison of the ethylene and NO densities between our simulations and simulations adopted from literature in Niessen et al.[34] and Shin et al.[33] for the same conditions. The left y-axis is for the comparison with the data of Niessen et al., whereas the comparison with the data of Shin et al. corresponds to the right y-axis.

work of Niessen et al.,[34] who investigated the influence of 2 000 ppm C$_2$H$_4$, 430 ppm NO and 70 ppm NO$_2$ in a 77:13:10 N$_2$/O$_2$/H$_2$O air mixture. A reasonable agreement for the density of C$_2$H$_4$ and NO is obtained, even at lower values of SED as compared to our own experiments. The bottom graph also presents results of Shin and Yoon[33] who investigated the influence of 500 ppm ethylene and 500 ppm NO in a gas mixture containing 90:10 N$_2$/O$_2$ and also in this case a reasonable agreement is reached.

To compare the results in terms of energy efficiency, Table 1 presents the amount of pollutant in ppm that can be converted for a SED of 1 mJ · cm^{-3} for different pollutants, together with the inlet concentration. Ethylene has similar energy efficiencies as trichloroethylene; however, for aromatic molecules the energy efficiency is typically a

Table 1. A comparison of the energy efficiency, in $ppm \cdot mJ^{-1} \cdot cm^3$, between different pollutants, as adopted from literature.

Type of pollutant	Inlet concentration [ppm]	Efficiency [$ppm \cdot mJ^{-1} \cdot cm^3$]	Reference
C_2H_4	500–13 700	3–5.5	This work
C_2HCl_3	500	15–20	[35]
C_6H_6	500–2 700	0.25–0.9	[38]
C_7H_8	150	0.5	[39]

The efficiency is calculated by dividing the converted concentration of the pollutant by the specific energy deposition.

factor of 10 lower. Indeed, benzene and toluene have a resonance system which makes the molecules much more stable compared with ethylene en trichloroethylene.

3.2. Effect of Concentration

In order to investigate the role of different species (i.e., radicals, metastables and electrons) in the initiation step of the destruction process, Figure 2 presents the relative contributions of these species, integrated over time during the pulse and afterglow, for a mixture of dry air with 10, 50, 100, 500, 1 000, 5 000 and 10 000 ppm ethylene, at a SED of 1 200 $mJ \cdot cm^{-3}$. The most important metastables playing a role in the destruction of ethylene are the $N_2(A^3\Sigma_u^+)$ species, whereas oxygen atoms are the most important radicals in the destruction process.

The constant line for electrons indicates a very low contribution (below 1%), independent of the concentration. Unlike the electrons, the relative importance of metastable nitrogen $N_2(A^3\Sigma_u^+)$ and atomic oxygen is influenced to some extent by the ethylene concentration. Below 100 ppm, a

Figure 2. Calculated relative contributions of radicals, metastables and electrons to the destruction of ethylene, as a function of the ethylene concentration in dry air at a SED of 600 $mJ \cdot cm^{-3}$.

constant ratio between the metastables and the radicals is found, with the latter being slightly more important in the destruction process. Between 100 and 1 000 ppm, a decrease in the relative contribution for the radicals and an increase for the metastables is observed. At around 1 000 ppm, the radicals and metastables appear to contribute to nearly the same extent to the destruction of ethylene. Finally, above 1 000 ppm, the relative contribution of the metastables further increases, whereas the radicals become gradually less important. This change in dominant destruction species upon increasing ethylene concentration suggests that the metastables, which have a shorter lifetime than the radicals now have a larger chance of reacting with the ethylene molecules. Further, it is clear from Figure 2 that the electrons are not suitable for the direct destruction of ethylene. It should be realized, however, that electron impact dissociation reactions become more important for concentrated systems, which are found, e.g., in the reforming of greenhouse gases.[40,41]

Some authors also indicated that electrons could play a role in the destruction in an indirect way.[42] For example, toluene could be ionized by electrons:[42]

$$C_6H_5CH_3 + e^- \rightarrow C_6H_5CH_3^+$$
$$k = 10^{-6} \, cm^3 \cdot molecule^{-1} \cdot s^{-1}$$
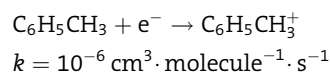
This ion can recombine with another electron to have a dissociative recombination:[42]

$$C_6H_5CH_3^+ + e^- \rightarrow C_6H_5 + CH_3$$
$$k = 10^{-7} \, cm^3 \cdot molecule^{-1} \cdot s^{-1}$$
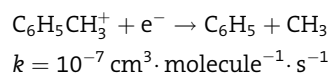
This process could explain the destruction of some aromatics: however, in the case of ethylene this destruction mechanism is not observed.

3.3. Effect of Specific Energy Deposition

We have also investigated the influence of SED on the initiation step, for a constant ethylene concentration of 500 ppm. The results shown in Figure 3 indicate the radicals as the dominant species at low values of SED; however, they
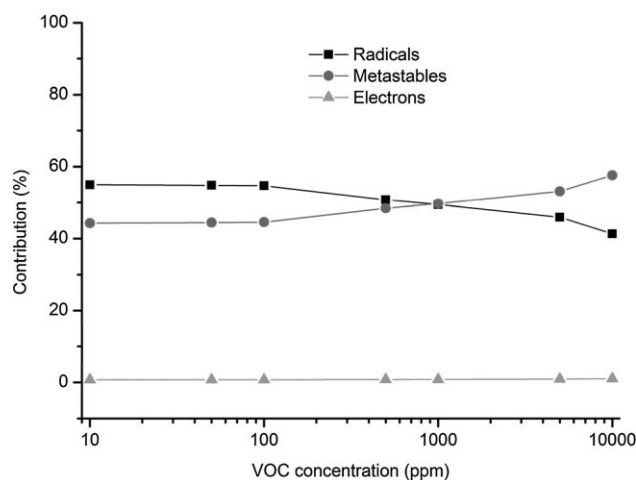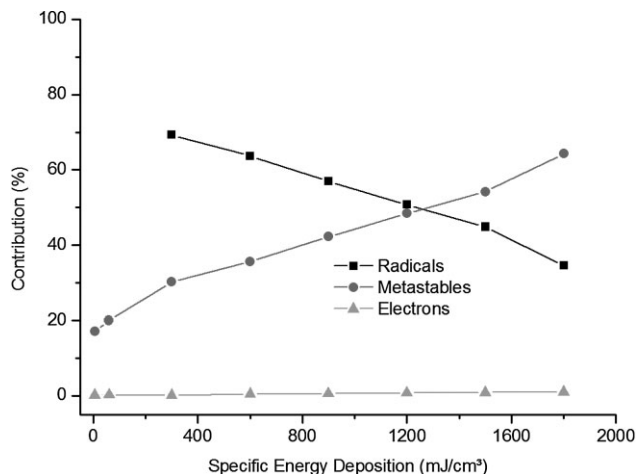
Figure 3. Calculated relative contribution of radicals, metastables and electrons to the destruction of ethylene, as a function of the SED in a dry air mixture containing 500 ppm ethylene.

Figure 4. Calculated relative contributions of the most important destruction reactions during the current pulse and the afterglow region, together with the corresponding total values (i.e., relative contributions of total destruction either during the pulse or afterglow, i.e., no. 5 and 11, respectively), for an ethylene concentration of 100 ppm and a SED of 600 mJ · cm^{-3}.

become clearly less important with increasing SED. At around 1 200 mJ/cm^3, the radicals and metastables appear to be equally important, and at still higher values of SED, the metastables become the dominant destruction species. The relative contribution of the electrons is below 1%, even at these high values of SED, which indicates that direct destruction by electrons is not important for the destruction of ethylene, even with concentrations of several thousands of ppm. The reason for this will be discussed below.

By increasing the SED more energy is introduced into the system, which is beneficial for the electron impact reactions. These reactions will produce more important destruction species, like atomic oxygen and nitrogen metastables; the latter becoming more important with increasing energy. Above 1 200 mJ · cm^{-3}, the production of metastables becomes dominant, so that more than half of the destruction is established by the metastables. Of course, at higher SED, the electrons will also be more energetic and in principle more capable for direct ethylene destruction. However, the metastables can transfer more energy to the ethylene molecules than the electrons, due to their higher mass.

3.4. Contribution of the Important Destruction Reactions

In order to obtain additional information about the important destruction pathways, the relative contributions of the most important destruction reactions during the current pulse and the afterglow, for 100 ppm ethylene at a SED of 600 mJ · cm^{-3}, are plotted in Figure 4. These conditions are used because they are suitable for industrial application of low temperature plasmas, as a result of the

low energy consumption and a corresponding simulated RE of 79%.

As is clear from this figure, the metastables, or more precisely the metastable nitrogen $N_2(A^3\Sigma_u^+)$ species, with a maximum density of 1.6×10^{16} cm^{-3}, are the dominant destruction species during the current pulse. The following reactions:[43,44]

$$C_2H_4 + N_2(A^3\Sigma_u^+) \rightarrow C_2H_2 + H_2 + N_2$$
$$k = 6.0 \times 10^{-11} \text{ cm}^3 \cdot \text{molecule}^{-1} \cdot \text{s}^{-1} \tag{1}$$

$$C_2H_4 + N_2(A^3\Sigma_u^+) \rightarrow C_2H_3 + H_2 + N_2$$
$$k = 4.0 \times 10^{-11} \text{ cm}^3 \cdot \text{molecule}^{-1} \cdot \text{s}^{-1} \tag{2}$$
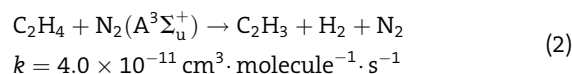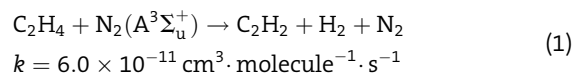
contribute together for 31% to the direct destruction of ethylene. Reaction (1) converts ethylene to acetylene, which is a more stable product than the vinyl radical formed by reaction (2), and therefore reaction (1) is slightly more important. The contribution of the electron impact dissociation reactions:[41]

$$C_2H_4 + e^- \rightarrow C_2H_2 + H_2 + N_2 \tag{3}$$

$$C_2H_4 + e^- \rightarrow C_2H_3 + H_2 + N_2 \tag{4}$$
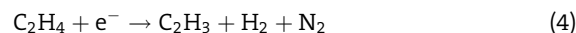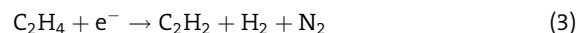
is <1%, as also indicated above.

The afterglow of the plasma is dominated by atomic oxygen species which have a density of approximately 1×10^{17} cm^{-3}. From the following reactions with atomic oxygen:[45]

$$C_2H_4 + O \rightarrow CH_2CHO + H$$
$$k = 2.8 \times 10^{-13} \text{ cm}^3 \cdot \text{s}^{-1} \tag{5}$$

$$C_2H_4 + O \rightarrow CH_2CO + H$$
$$k = 3.8 \times 10^{-14}\ cm^3 \cdot s^{-1} \tag{6}$$

$$C_2H_4 + O \rightarrow CHO + CH$$
$$k = 4.9 \times 10^{-13}\ cm^3 \cdot s^{-1} \tag{7}$$

$$C_2H_4 + O \rightarrow CH_2O + CH$$
$$k = 8.3 \times 10^{-12}\ exp(-754/T_g)\ cm^3 \cdot s^{-1} \tag{8}$$

$$C_2H_4 + O \rightarrow C_2H_3 + OH$$
$$k = 1.3 \times 10^{-12}\ (T_g/300)$$
$$exp(-1\,880/T_g)\ cm^3 \cdot s^{-1} \tag{9}$$
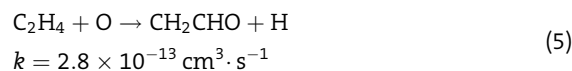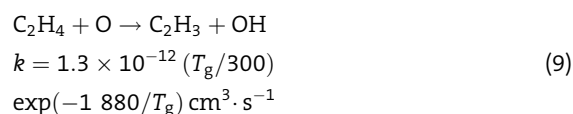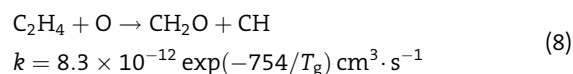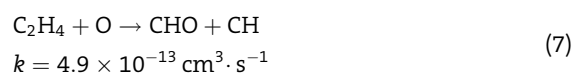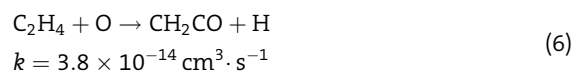
reaction (8) is the most important destruction process, with a contribution of 28%. Also reactions (5) and (7) are quite important, with a contribution of 18 and 20%, respectively. Formaldehyde is a major product in the destruction of ethylene, not only because it is created in reaction (8), but also because the products formed in reactions (5), (6), (7) and (9) will eventually react to formaldehyde. When we look at the complete destruction process, the afterglow is responsible for ±68% of the total destruction process, which is dominated by atomic oxygen.

As indicated in the beginning of the paper, a further increase of their relative contribution might be expected when simulating multiple pulses, which can cause accumulation of certain radicals in each pulse and induce a further increase of their relative contribution. This destruction pathway is also indicated to be the most important one by other authors for different VOCs (i.e., trichloroethylene, acetaldehyde and formaldehyde).[35,46,47] However, we would like to stress that other pathways, i.e., with ozone or hydroxyl radicals, which are also reported to be important in VOC destruction literature, are not found in our simulations, for the following reasons.[48,49]

The reaction rate coefficients for the reactions of ozone with VOCs are rather small, as is illustrated here for ethylene and toluene:[50,51]

$$O_3 + C_2H_4 \rightarrow products$$
$$k = 1.68 \times 10^{-18}\ cm^3 \cdot s^{-1}\ at\ 298\,K$$

$$O_3 + C_7H_8 \rightarrow products$$
$$k = < 1 \times 10^{-21}\ cm^3 \cdot s^{-1}\ at\ 298\,K$$
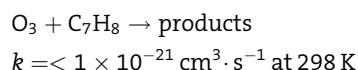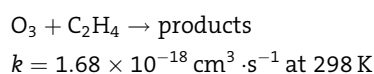
Indeed, the reaction rate coefficients for the corresponding reactions with atomic oxygen are much higher:[52,53]

$$O + C_2H_4 \rightarrow products$$
$$k = 7.51 \times 10^{-13}\ cm^3 \cdot s^{-1}\ at\ 298\,K$$

$$O + C_7H_8 \rightarrow products$$
$$k = 2.32 \times 10^{-13}\ cm^3 \cdot s^{-1}\ at\ 298\,K$$
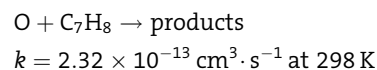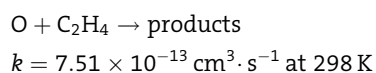
However, not only the rate coefficients control the destruction rate of ethylene but also the density of the reacting species. Obviously, it is the product of rate coefficient and species densities which determines the rate. Although the maximum density of ozone ($7 \times 10^{16}\ cm^{-3}$) is only slightly lower than the maximum density of atomic oxygen ($2 \times 10^{17}\ cm^{-3}$), the time-integrated absolute contribution, yields a value of $10^{10}\ cm^{-3}$, which is significantly smaller than for atomic oxygen, i.e., $10^{14}\ cm^{-3}$, in our simulations with ethylene. Therefore, our simulations do not indicate ozone as one of the dominant species in the destruction process. On the other hand, the reactions with the hydroxyl radicals are characterized by a reaction rate coefficient that is even one order of magnitude higher than for atomic oxygen as illustrated below:[54,55]

$$OH + C_2H_4 \rightarrow products$$
$$k = 8.51 \times 10^{-12}\ cm^3 \cdot s^{-1}\ at\ 298\,K$$

$$OH + C_7H_8 \rightarrow products$$
$$k = 5.60 \times 10^{-12}\ cm^3 \cdot s^{-1}\ at\ 298\,K$$
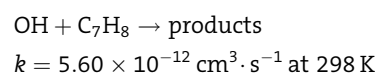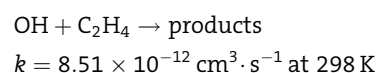
However, the density of the hydroxyl radicals was found to be at least two orders of magnitude lower in our simulations than the density of atomic oxygen (i.e., in the order of $10^{15}\ cm^{-3}$ vs. $10^{17}\ cm^{-3}$), at least in dry air. Therefore, the time-integrated absolute contribution yields a value of $10^9\ cm^{-3}$, which is significantly smaller than for atomic oxygen, i.e., $10^{14}\ cm^{-3}$.

4. Conclusion

We have demonstrated by means of modelling that direct electron impact dissociation reactions are negligible for the destruction of ethylene in the range of 10–10 000 ppm and 0–3 000 mJ·cm^{-3}. The radicals appear to be the dominant destruction species at low ethylene concentrations and low values of SED, whereas at high concentrations and high values of SED, the metastables are found to dominate the destruction process. The simulations also showed that quenching reactions with metastable nitrogen $N_2(A^3\Sigma_u^+)$ appear to be an important destruction process of ethylene besides the reactions with radicals.

Finally, we found that atomic oxygen is the dominant destruction species in dry air, at low values of SED and low ethylene concentrations, which are typically applied for industrial applications. Our future work will be to investigate the addition of water, defining the complete

destruction pathway in humid air, as well as the effect of multiple pulses which is closer to reality for practical DBD.

[1] H. L. Chen, H. M. Lee, S. H. Chen, M. B. Chang, S. J. Yu, S. N. Li, *Environ. Sci. Technol.* **2009**, *43*, 2216.

[2] J. Vandurme, J. Dewulf, C. Leys, H. Vanlangenhove, *Appl. Catal. B* **2008**, *78*, 324.

[3] J. C. Whitehead, *Pure Appl. Chem.* **2010**, *82*, 1329.

[4] A. M. Harling, A. E. Wallis, J. C. Whitehead, *Plasma Process. Polym.* **2007**, *4*, 463.

[5] B. Eliasson, U. Kogelschatz, *IEEE Trans. Plasma Sci.* **1991**, *19*, 1063.

[6] B. Eliasson, W. Egli, U. Kogelschatz, *Pure Appl. Chem.* **1994**, *66*, 1275.

[7] I. Traus, H. Suhr, *Plasma Chem. Plasma Process.* **1992**, *12*, 275.

[8] I. Sardja, S. K. Dhali, *Appl. Phys. Lett.* **1989**, *56*, 21.

[9] S. K. Dhali, I. Sardja, *J. Appl. Phys.* **1991**, *69*, 6319.

[10] M. B. Chang, M. J. Kushner, M. J. Rood, *Plasma Chem. Plasma Process.* **1992**, *12*, 565.

[11] U. Kogelschatz, *Plasma Chem. Plasma Process.* **2003**, *23*, 1.

[12] K. Urashima, K. G. Kostov, C. Jen-Shih, Y. Okayasa, T. Iwaizumi, K. Yoshimura, T. Kato, *Ind. Appl. 200*, 37. **1456**.

[13] H. H. Kim, Y. H. Lee, A. Ogata, S. Futamura, *Catal. Commun.* **2003**, *4*, 347.

[14] A. A. H. Mohamed, R. H. Stark, J. H. Yuan, K. H. Schoenbach, *IEEE Trans. Plasma Sci.* **2005**, *33*, 1416.

[15] R. K. Janev, D. Reiter, *ChemInform* **2003**, *34*, 25.

[16] Y. Xu, L. Jia, M. Ge, L. Du, G. Wang, D. Wang, *Chin. Sci. Bull.* **2006**, *51*, 2839.

[17] S. Chavadej, K. Saktrakool, P. Rangsunvigit, L. Lobban, T. Sreethawong, *Chem. Eng. J.* **2007**, *132*, 345.

[18] A.-M. Zhu, Q. Sun, J.-H. Niu, Y. Xu, Z.-M. Song, *Plasma Chem. Plasma Process.* **2005**, *25*, 371.

[19] L. D. Cloutman, *A Selected Library of Transport Coefficients for Combustion and Plasma Physics Applications*. Lawrence Livermore National Laboratory report, UCRL-ID-139893, 2000.

[20] W.-J. Liang, J. Li, J.-X. Li, T. Zhu, Y.-Q. Jin, *J. Hazard. Mater.* **2010**, *175*, 1090.

[21] H. Huang, D. Ye, D. Y. C. Leung, F. Feng, X. Guan, *J. Mol. Catal. A: Chem.* **2011**, *336*, 87.

[22] A. S. Chiper, N. Blin-Simiand, M. Heninger, H. Mestdagh, P. Boissel, F. Jorand, J. Lemaire, J. Leprovost, S. Pasquiers, G. Popa, C. Postel, *J. Phys. Chem. A* **2010**, *114*, 397.

[23] N. Blin-Simiand, F. Jorand, L. Magne, S. Pasquiers, C. Postel, J. R. Vacher, *Plasma Chem. Plasma Process.* **2008**, *28*, 429.

[24] Y. S. Mok, V. Demidyuk, J. C. Whitehead, *J. Phys. Chem. A* **2008**, *112*, 6586.

[25] M. J. Kushner, *J. Appl. Phys.* **1993**, *73*, 51.

[26] I. Orlandini, U. Riedel, *J. Phys. D: Appl. Phys.* **2000**, *33*, 2467.

[27] C. Fitzsimmons, F. Ismail, J. C. Whitehead, J. J. Wilman, *J. Phys. Chem. A* **2000**, *104*, 6032.

[28] V. Demidyuk, S. L. Hill, J. C. Whitehead, *J. Phys. Chem. A* **2008**, *112*, 7862.

[29] S. L. Hill, J. C. Whitehead, K. Zhang, *Plasma Process. Polym.* **2007**, *4*, 710.

[30] L. Magne, S. Pasquiers, N. Blin-Simiand, C. Postel, *J. Phys. D: Appl. Phys.* **2007**, *40*, 3112.

[31] R. Dorai, M. J. Kushner, *J. Appl. Phys.* **2000**, *88*, 3739.

[32] M. Hübner, J. Röpcke, *J. Phys.: Conf. Ser.* **2009**, *157*, 012004.

[33] H. H. Shin, W. S. Yoon, *Plasma Chem. Plasma Process.* **2003**, *23*, 681.

[34] W. Niessen, O. Wolf, R. Schruft, M. Neiger, *J. Phys. D: Appl. Phys.* **1998**, *31*, 542.

[35] D. Evans, L. A. Rosocha, G. K. Anderson, J. J. Coogan, M. J. Kushner, *J. Appl. Phys.* **1993**, *74*, 5378.

[36] R. Dorai, M. J. Kushner, *J. Phys. D: Appl. Phys.* **2001**, *34*, 574.

[37] X. Tu, H. J. Gallon, M. V. Twigg, P. A. Gorry, J. C. Whitehead, *J. Phys. D: Appl. Phys.* **2011**, *44*, 274007.

[38] M. P. Cal, M. Schluep, *Environ. Prog.* **2001**, *20*, 151.

[39] H. H. Kim, A. Ogata, S. Futamura, *Appl. Catal. B Environ.* **2008**, *79*, 356.

[40] C. De Bie, B. Verheyde, T. Martens, J. van Dijk, S. Paulussen, A. Bogaerts, *Plasma Process. Polym.* **2011**, *8*, 1033.

[41] H. Kohno, A. A. Berezin, J. S. Chang, M. Tamura, T. Yamamoto, A. Shibuya, S. Hondo, *ITIA* **1998**, *34*, 953.

[42] C. De Bie, T. Martens, J. van Dijk, S. Paulussen, B. Verheyde, S. Corthals, A. Bogaerts, *Plasma Sources Sci. Technol.* **2011**, *20*, 024008.

[43] N. Moreau, S. Pasquiers, N. Blin-Simiand, L. Magne, F. Jorand, C. Postel, J.-R. Vacher, *J. Phys. D: Appl. Phys.* **2010**, *43*, 285201.

[44] H. Umemoto, *J. Chem. Phys.* **2007**, *127*, 014304.

[45] D. L. Baulch, C. J. Cobos, R. A. Cox, C. Esser, P. Frank, T. Just, J. A. Kerr, M. J. Pilling, J. Troe, R. W. Walker, J. Warnatz, *J. Phys. Chem. Ref. Data* **1992**, *21*, 411.

[46] H. M. Lee, M. B. Chang, *Plasma Chem. Plasma Process.* **2001**, *21*, 329.

[47] W. Liang, J. Li, J. Li, Y. Jin, *J. Hazard. Mater.* **2009**, *170*, 633.

[48] S. Schmid, M. C. Jecklin, R. Zenobi, *Chemosphere* **2010**, *79*, 124.

[49] Y. Guo, X. Liao, J. He, W. Ou, D. Ye, *Catal. Today* **2010**, *153*, 176.

[50] R. Atkinson, D. L. Baulch, R. A. Cox, J. N. Crowley, R. F. Hampson, R. G. Hynes, M. E. Jenkin, M. J. Rossi, J. Troe, *Atmos. Chem. Phys.* **2004**, *4*, 1461.

[51] D. H. Stedman, H. Niki, *Environ. Lett.* **1973**, *4*, 303.

[52] D. Baulch, C. Cobos, R. Cox, P. Frank, G. Hayman, T. Just, J. Kerr, T. Murrells, M. Pilling, J. Troe, R. W. Walker, J. Warnatz, *J. Phys. Chem. Ref. Data* **1994**, *23*, 847.

[53] J. T. Herron, R. E. Huie, *J. Phys. Chem. Ref. Data* **1973**, *2*, 467.

[54] R. Atkinson, *Chem. Rev.* **1986**, *86*, 69.

[55] B. J. Finlayson-Pitts, S. K. Hernandez, H. N. Berko, *J. Phys. Chem* **1993**, *97*, 1172.